The m6A demethylase FTO promotes esophageal cancer progression via the YTHDF1/AKT3 signaling network

Ran Wei
The First Affiliated Hospital of USTC: Anhui Provincial Hospital
Fangfang Zhao
The First Affiliated Hospital of USTC: Anhui Provincial Hospital
Zhenyu Li
Wannan Medical College
Lingsuo Kong
The First Affiliated Hospital of USTC: Anhui Provincial Hospital
Yuanhai Li
Anhui Medical College: Anhui Medical University
Chunbao Zang (zangchunbao@ustc.edu.cn)
The First Affiliated Hospital of USTC: Anhui Provincial Hospital

Research

Keywords: esophageal cancer, N6-methyladenosine (m6A), FTO, AKT3, YTHDF1

Posted Date: June 21st, 2022

DOI: https://doi.org/10.21203/rs.3.rs-1731913/v1

Abstract

Background

As the most abundant modification in eukaryotic messenger RNAs (mRNAs), the N^6-methyladenosine (m^6A) plays vital roles in many biological processes.

Results

Here we applied the methylated RNA immunoprecipitation sequencing (MeRIP-seq) and transcriptomic RNA sequencing (RNA-seq) to screen the m^6A targets in esophageal cancer patients. We found that the m^6A demethylase FTO was significantly up regulated in esophageal cancer cell lines and patient tissues. *In vivo* and *in vitro* assays demonstrated that FTO was involved in the proliferation, migration, invasion, and apoptosis of esophageal cancer cells. Moreover, we found that the m^6A methyltransferase METTL14 negatively regulates FTO function on esophageal cancer progression. By using transcriptome-wide m^6A-seq and RNA-seq assays, we identified that *AKT3* is a downstream target of FTO, which acts in concert to regulate the tumorigenesis and metastasis of esophageal cancer.

Conclusions

All these findings revealed insights into the m^6A-regulated tumorigenesis in esophageal cancer, which is applicable for designing new therapeutic strategy.

Introduction

The mRNA m^6A modification was identified in the 1970s [1, 2] and is the most abundant in eukaryotic mRNAs with unique distribution patterns [3]. In mammalian cells, the m^6A modification is catalyzed by a methyltransferase complex (“writers”) consisting of the proteins methyltransferase-like 3 (METTL3), METTL14, Wilms tumor 1 associated protein (WTAP), VIRMA (KIAA1429), and RBM15 [4, 5]. Notably, the first RNA demethylase, fat mass and obesity-associated protein (FTO), was identified to function as an m^6A “eraser” to remove m^6A modification from RNA, revealing that RNA modification is reversible [6]. Afterwards, the alkylation repair homolog protein 5 (ALKBH5) was proven to be another “eraser” of m^6A modification [7], indicating a dynamic nature of m^6A methylation. Since then, numerous studies have focused on the dynamics of m^6A modification [8–12]. Moreover, m^6A-binding proteins with a YTH domain, including the cytoplasmic proteins YTHDF1, YTHDF2, and YTHDF3 and the nuclear protein YTHDC1, have been identified as the “readers” of m^6A and modulate mRNA stability and translation [9, 10, 13, 14].

Recently, accumulated studies have focused on the biological functions of m^6A modification in mRNA [15]. It has been reported that m^6A modification is involved in various biological processes, including the heat-shock response [13], DNA damage response [16, 17], mRNA clearance [8], neuronal functions [18], cortical neurogenesis [19], progenitor cell specification [20], and T cell homeostasis [21]. Moreover, m^6A modification has been found to be associated with the tumorigenesis and progression of various cancers [22].

The m^6A demethylase FTO was found to play critical roles in regulating fat mass, adipogenesis, and body weight [23–25]. In addition, large-scale epidemiological studies have demonstrated the association of the FTO SNP risk genotype with the development of cancers such as breast, kidney, prostate, and pancreatic cancers, as well as leukemia, lymphoma and myeloma [26–28]. Some studies have shown that FTO plays a carcinogenic role in esophageal cancer and other solid tumors [29–31]. A previous study showed that FTO plays an oncogenic role in cell transformation and leukemogenesis [32]. However, the definitive role of FTO in cancer remains limited.

In this study, we systematically investigated the role of m^6A modification in the tumorigenesis of esophageal cancer, which remains one of the most common forms of cancer worldwide [33, 34]. We found a significantly increased level of FTO in esophageal cancer cells. The following functional studies revealed an oncogenic role of FTO in esophageal cancer tumorigenesis. Moreover, we found that the m^6A methyltransferase METTL14 is also involved in FTO-regulated m^6A modification, which acts in concert with FTO to regulate AKT3 methylation in the tumorigenesis and metastasis of esophageal cancer.

Results

FTO expression is upregulated in esophageal cancer

We first investigated the m^6A levels in the mRNAs of esophageal cancer cells. By using MeRIP-PCR, we identified that the m^6A levels of mRNAs isolated from five esophageal cancer cell lines were statistically ($p < 0.05$, *t* test) less abundant than those of one normal control cell line (Fig. 1A). The m^6A/A level of mRNA is decreased to ~ 10% in esophageal cancer cells compared with ~ 40% in normal cells (Fig. 1A). These results indicate that m^6A in mRNAs should be demethylated in esophageal cancer cells. We thus detected the expression of the N^6-methyladenosine RNA demethylase FTO in the tissues of different esophageal cancer patients. Compared to normal tissues, tissues from esophageal cancer patients had an upregulated level of FTO expression (Fig. 1B). Moreover, esophageal cancer patients with higher FTO expression had shorter overall survival (Fig. 1C), which suggests that FTO expression might serve as a prognostic marker for esophageal cancer patients. The subsequent western blotting analysis also showed significantly higher expression of FTO in esophageal cancer cells, especially in KYSE150 cells, than in normal esophageal cells (Fig. 1D). In addition, the esophageal cancer patients had a higher expression of FTO proteins, as analyzed by western blotting (Fig. 1E). The expression of FTO was also significantly higher in esophageal cancer patient tissues than in paracancerous tissues (PT) (Fig. 1F).

Collectively, these results clearly demonstrated that FTO is highly expressed in esophageal cancer patients, which correlates with a lower survival rate of esophageal cancer patients.

FTO is involved in the proliferation, migration, invasion, and apoptosis of esophageal cancer cells

To investigate the potential roles of FTO in EC cells, we performed a series of functional assays to characterize the effect of FTO in EC cells. We first down regulated the expression of FTO by transfection of FTO sh-RNAs in KYSE150 cells (Fig. 2A). The following CCK-8 assays showed that down regulation of FTO significantly inhibited the proliferation of KYSE150 cells (Fig. 2B). Moreover, FTO knockdown in KYSE150 cells decreased the cell migration and invasion capability compared to that of the control cells (Fig. 2C). Previous studies have shown that E-cadherin is a biomarker for cell migration [35, 36]; thus, we detected the expression of E-cadherin in FTO knockdown cells. The results showed that down regulation of FTO correlates with the higher expression of E-cadherin (E-cad) in KYSE150 cells (Fig. 2D), indicating that FTO might be associated with E-cadherin-regulated cell migration in esophageal cancer cells.

Afterwards, we overexpressed FTO in HEECs by transfection of FTO-overexpressing lentivirus (Fig. 2E). The cell proliferation rate was significantly increased upon overexpression of FTO in HEECs (Fig. 2F). Moreover, the cell migration and cell invasion capabilities were also increased in FTO-overexpressing HEEC cells (Fig. 2G). In addition, the colony formation assays showed that compared to the control cells, FTO overexpression significantly promoted cell proliferation in KYSE150 cells, whereas FTO knockdown largely impeded cell proliferation (Fig. 2H). Moreover, compared to the control cells, FTO overexpression in HEEC cells drastically decreased the apoptotic cells from 25–10%, as analyzed by flow cytometry (Fig. 2I), indicating a decreased cell apoptosis rate with FTO overexpression. All these results indicated that the oncogenic role of FTO is involved in cell proliferation, migration, invasion, and cell apoptosis in esophageal cancer cells.

FTO negatively correlates with METTL14 in esophageal cancer cells

Our results showed that a higher FTO level correlates with a poor prognosis in ES patients (Fig. 1C). To further characterize whether m^6A methylation is indeed associated with ES prognosis, we introduced the ratio of FTO/METTL14 to represent the methylation rate in the cells. Given that METTL14 is a well-characterized m^6A methyltransferase [37, 38], a higher FTO/METTL14 ratio represents a lower level of m^6A methylation in cells. Analysis of ES patients with higher FTO/METTL14 ratios showed a rather poor prognosis rate compared to that of patients with lower FTO/METTL14 ratios (Fig. 3A). Further analysis of the differentially expressed genes by RNA-seq showed that FTO overexpression and METTL14 overexpression resulted in a total of 157 shared differentially expressed genes (Fig. 3B). These results indicated that FTO might be functionally associated with METTL14. To further examine the correlation

between FTO and METTL14, we compared the proliferation ability of KYSE150 cells with the reversal changes of FTO or METTL14. As expected, down regulation of FTO or up regulation of METTL14 reduced the proliferation ability, which could be restored via down regulation of METTL14 (Fig. 3C). Moreover, the decreased migration or invasion of KYSE150 cells via FTO knockdown could also be restored by METTL14 overexpression (Fig. 3D). In contrast, METTL14 knockdown has the opposite effect of an elevated capability of migration or invasion in KYSE150 cells. All these results suggest that FTO and METTL14 negatively correlate with each other in functioning as biomarkers in esophageal cancer patients.

Akt3 is regulated by FTO-mediated m^{6}A modification in esophageal cancer cells

To investigate the potential role of FTO in tumor progression, we detected the m^{6}A contents of the total mRNA with the EpiQuik™ m^{6}A RNA Methylation Quantification Kit (Colorimetric) in FTO-overexpressing HEEC and FTO-silenced KYSE150 cells. As expected, FTO overexpression significantly decreased the m^{6}A content in HEECs, whereas FTO silencing dramatically increased the m^{6}A content in KYSE150 cells (Figs. 4A-4B). As analyzed by the RMBase database, the genes with m^{6}A modification have a consensus motif of U/AGGAC (Fig. 4C), which is the common feature among the genes with m^{6}A methylation [39, 40].

We take the intersection of the down-regulated peak after overexpression of FTO and the up-regulated peak after interference with FTO, and then enrich the KEGG function of the intersected genes. The results show that cell cycle and other pathways are significantly enriched in the genes with different peaks. Compared to the control cells, 128 genes showing a 1.5-fold m^{6}A change in the expression level were identified in esophageal cancer cells. Kyoto Encyclopedia of Genes and Genomes (KEGG) enrichment analysis indicated that a handful of genes were associated with the different metabolic pathways in various cancer cells. The overall level analysis of the m^{6}A modification after FTO knockout indicated that FTO was related to the methylation of m^{6}A (Fig. 4D). Among these genes, we selected the top seven most differentially expressed members and detected their expression in KYSE150 cells by real-time PCR. The results showed that METTL1, CAMKK1, PKN2, and TGFBR1 were upregulated in FTO-silenced KYSE150 cells, whereas ERBB2, AKT3 and PAK1P1 were downregulated (Fig. 4E). Among the three downregulated genes, *Akt3*, which is a serine/throne kinase from the *Akt* family [41, 42], is involved in the biogenesis of many different types of cancers [43]. The correlation prediction of FTO and AKT3 by the GEPIA database gave an R-value of 0.55, which strongly indicated the physical interaction between *Fto* and *Akt3* genes, the correlation of genes suggests that the two proteins may have some physical interaction (Fig. 4F). We thus detected the m^{6}A abundance on *Akt3* mRNA transcripts in KYSE30 and KYSE150 cells by m^{6}A-seq, and the results showed that m^{6}A methylation was enriched in the exon and 3'UTR regions of *Akt3* with a clustered distribution (Fig. 4G).

To further investigate the role of *Akt3* in FTO-regulated m^{6}A methylation, we detected the m^{6}A content in KYSE150 cells by MeRIP-PCR. The results showed that *FTO* knockdown retained the m^{6}A methylation in *Akt3*, as shown by an elevated m^{6}A content in KYSE150 cells (Figs. 4H and 4I). To examine the role of m^{6}A methylation on the *Akt3* 3'UTR, containing firefly' luciferase reporters were generated, followed by the wild-type *Akt3* 3'UTR, mutant1 or mutant2 3'UTR. The 3'UTR-reporter luciferase assay showed that compared to the control cells, the mutant1 3'UTR slightly but not significantly reduced *Akt3* expression, whereas the mutant2 3'UTR had a minor effect on *Akt3* expression (Fig. 4J). Dot plot analysis of the overall level of m^{6}A modification in esophageal cancer cells before and after knockdown of the *Akt3* m^{6}A modification site. The results indicated that m^{6}A methylation of the 3'UTR might not be involved in the m^{6}A modification-regulated *Akt3* expression.

AKT3 is involved in m^{6}A-regulated esophageal cancer tumorigenesis and metastasis

We then characterized the roles of *Akt3* in esophageal cancer cell functions by several *in vitro* experiments. Notably, overexpression of FTO in HEEC cells largely increased the expression of both *Akt3* mRNA and protein (Fig. 5A), whereas FTO knockdown in KYSE150 cells decreased the expression of *Akt3* mRNA and protein (Fig. 5B). To further investigate whether FTO affects the stability of *Akt3* mRNA, we tested *AKT3* mRNA levels in KYSE150 cells with FTO knockdown after treatment with actinomycete D, which is ametabolic inhibitor [35, 44]. The results showed that the mRNA level dramatically decreased overtime with FTO knockdown (Fig. 5C), indicating that FTO might increase the stability of *Akt3* mRNA, which results in a higher level of AKT3 protein expression.

Next, we downregulated AKT3 expression in KYSE150 cells and tested its effect on KYSE150 cellular functions. Transfection of either of the three AKT3 siRNAs in KYSE150 cells significantly decreased the expression of AKT3 at both the mRNA and protein levels (Fig. 5D). In addition, overexpression of AKT3 also increased the expression of Vimentin (Fig. 5E), indicating that AKT3 promotes tumor cell migration. Accompanied by the decrease in AKT3 with si-AKT3 transfection in KYSE150 cells, the cell proliferation ratio also decreased over time (Fig. 5F). Moreover, the cell invasion and migration capabilities were also decreased with AKT3 knockdown in KYSE150 cells (Fig. 5G). All these results indicated that *AKT3* is involved in the tumorigenesis of esophageal cancer progression.

FTO and AKT3 act in concert to regulate esophageal cancer cell tumorigenesis and metastasis

To further investigate the correlation between FTO and AKT3 in esophageal cancer tumorigenesis, we overexpressed AKT3 in KYSE150 cells accompanied by FTO knockdown. As shown in Fig. 6A, compared to the transfection of AKT3-overexpressing vector (AKT3-OE), which increased *AKT3* mRNA expression ~

43.5-fold, AKT3 expression in FTO-silenced KYSE150 cells transfected with AKT3-overexpressing vector (sh-FTO + AKT3-OE) increased ~ 15.3-fold, which largely compromised the upregulation of *AKT3* mRNA. The results also coincide with the notion that FTO-regulated m^{6}A demethylation promotes *AKT3* mRNA stability (Fig. 5C). As a result, the AKT3 protein levels were also upregulated in the AKT3-OE and sh-FTO + AKT3-OE KYSE150 cells (Fig. 6B) but were slightly lower in the sh-FTO + AKT3-OE cells. To test whether AKT3 could restore the effect of FTO knockdown, we tested the proliferation ratio of KYSE150 cells using CCK-8 assays. The results showed that FTO knockdown decreased the proliferation ratio, which could be restored by AKT3 overexpression in sh-FTO + AKT3-OE cells (Fig. 6C). Similarly, wound healing, migration, invasion and colony formation assays showed that the effects of FTO knockdown in KYSE150 cells could also be restored by AKT3 overexpression (Figs. 6D-6G). These results also indicated that FTO-regulated m^{6}A demethylation of AKT3 is associated with the tumorigenesis and metastasis of esophageal cancer cells.

YTHDF1 maintains AKT3 mRNA stability in an m^{6}A-dependent manner

Previous studies have identified two major families of m^{6}A “readers” that might play a specific role in controlling the fate of methylated mRNAs, such as the YTH family and the IGF2BP family [5, 45, 46]. To identify the specific m^{6}A readers of *AKT3* and determine the m^{6}A-dependent mechanism of *AKT3* regulation, we performed FLAG RNA pull-down assays in KYSE150 cells to screen *AKT3*-related m^{6}A readers. Notably, YTHDC1 and YTHDF1, but not other members in the YTH family, specifically bind to the *AKT3* full-length transcripts in KYSE150 cells (Fig. 7A). Biotin-based pull-down assays also confirmed the direct interactions of *AKT3* mRNA with both YTHDC1 and YTHDF1 (Figs. 7B-7C), indicating a potential positive regulatory mechanism. Further detection of the expression levels in the tumor tissues compared to the control groups revealed that only YTHDF1 had an upregulated expression level in esophageal cancer cells (Fig. 7D). In contrast, YTHDC1 showed no significant changes in the expression level compared to the control groups (Fig. 7E).

To further test the role of YTHDF1 in AKT3 stability, we inhibited or increased the expression of YTHDF1 in KYSE150 cells. As a result, AKT3 mRNA and protein expression were decreased upon the overexpression of YTHDF1 in KYSE150 cells (Fig. 7F). Moreover, *AKT3* mRNA and protein expression were upregulated after siRNA inhibition of YTHDF1 in KYSE150 cells (Fig. 7G). Taken together, our results suggested that the methylated *AKT3* transcripts might be directly recognized by YTHDF1, which maintained the stability of the *AKT3* transcripts.

FTO and AKT3 promote esophageal cancer progression in vivo

To test the potential role of FTO and AKT3 in esophageal cancer biogenesis *in vivo*, we injected sh-FTO or AKT3-OE KYSE150 cells subcutaneously into nude mice. Then, the mice were killed when the tumor volumes were approximately 1000 mm^3 for each group. Compared to the control groups, transfection of sh-FTO KYSE150 cells significantly decreased the tumor weight, whereas transfection of AKT3-OE KYSE150 cells increased the tumor weight (Fig. 8A). To further determine the impacts of m^6A methylation on *in vivo* metastasis, sh-FTO, AKT3-OE or sh-FTO & AKT3-OE KYSE150 cells were injected into nude mice by tail vein injection to analyze lung colonization. As shown in Figure. 8B, the number of lung tumors derived from FTO knockdown KYSE150 cells showed no significant changes; however, AKT3-OE or sh-FTO&AKT3-OE significantly promoted the number of lung tumors compared with control cells, suggesting that AKT3 overexpression promoted tumor metastasis *in vivo*. All these results suggested that FTO and AKT3 are involved in esophageal cancer progression *in vivo*.

Discussion

Increasing evidence indicates that mRNA m^6A modification participates in a number of biological functions and in the progression of cancer cells [32, 35, 47]. In this study, we demonstrated that mRNA m^6A modification can regulate the progression of esophageal cancer. In brief, the expression level of FTO in esophageal cancer cells was negatively correlated with the m^6A levels in mRNA. Changes in FTO and METTL14 levels largely affect the *in vitro* proliferation, migration, and invasion of cancer cells. Further investigations identified *AKT3* as one of the targets of FTO. In particular, AKT3 is a phosphatidylinositol-3-kinase, and the protein kinase B family is a key element of the PI3K/AKT signaling pathway. The AKT pathway was found to regulate many hallmarks of cancer and the metastatic cascade in breast cancer [48–50]. In addition, much effort has been made to develop targeted therapies for AKT signaling in breast cancer [51–53]. Thus, the PI3K/AKT pathway is a promising target for cancer therapy owing to the high frequency of its dysregulation in human breast cancer [54]. Here, we showed that *AKT3* is involved in the progression of esophageal cancer, which provides the basis for further targeting the *AKT3* pathway for clinical therapy of esophageal cancer.

Knowledge of the roles of mRNA modification in controlling cancer progression remains limited. As the first characterized m^6A demethylase, FTO has been reported to regulate the tumorigenesis of different types of cancers. FTO was found to enhance leukemic oncogene-mediated cell transformation and leukemogenesis by reducing the m^6A levels of its targets [32]. In addition, pharmaceutical inhibition of FTO by a chemical inhibitor Inhibit tumor progression and significantly prolong the life of glioblastoma stem cell transplanted mice [47]. On the other hand, METTL14, which is the methyltransferase of mRNA m^6A, exhibits several functions in cancer cells, such as regulating leukemogenesis and proliferation of hematopoietic stem/progenitor cells (HSPCs) [38]. Targeting METTL14, especially combined with differentiation inducers, may be an effective new therapeutic strategy for the treatment of AML. In addition, METTL14 and METTL3 form a stable heterodimer core complex and play a role in cell m^6A deposition, which can inhibit the metastatic potential by regulating primary microRNA 126 treatment in an m^6A dependent manner [55]. In this study, we provided a link between the regulation of *AKT3* mRNA

m^{6}A methylation by FTO and METTL14. We found that downregulation of FTO or overexpression of METTL14 have a similar effect on multiple aspects of esophageal cancer progression, including migration, invasion, proliferation, and tumorigenesis, which also suggests that FTO function could be restored by METTL14 in esophageal cancer. Our results describe the roles of m^{6}A and FTO in cancer progression and provide a basis for the development of therapeutic strategies against esophageal cancer metastasis. Notably, the METTL14/FTO/AKT3 signaling network might have other normal functions in addition to influencing tumorigenesis in esophageal cancer. More investigations are needed to clarify the fine regulatory circuit of these players in cellular functions.

The m^{6}A modification modulates all stages in the life cycle of RNA, such as RNA processing, nuclear export, and translation modulation [14, 56, 57]. For example, m^{6}A modification can promote the de alkenylation of RNA through the first characterized m6A "reader" protein YTHDF2, thereby triggering mRNA degradation [9]. Here, we showed that the stability of *AKT3* mRNA transcripts is enhanced by the reader protein YTHDF1. Previous studies have shown that YTHDF1 is linked to the progression of various cancers, including non-small-cell lung cancer [58], colorectal carcinoma [59], and ovarian cancer [60]. In our study, we found that knockdown of YTHDF1 decreased *AKT3* at both the mRNA and protein levels (Fig. 7F), whereas YTHDF1 overexpression significantly enhanced *AKT3* mRNA and protein levels. These data support that *AKT3* is the direct target of YTHDF1 in esophageal cancer. The results indicated that YTHDF1 might regulate the transcription and translation of *AKT3*. However, the detailed mechanism by which YTHDF1 regulates *AKT3* expression needs further investigation.

In conclusion, we provide a large amount of in vitro and in vivo evidence that m^{6}A modification can regulate the progression of esophageal cancer by promoting the growth, survival and invasion of cancer cells. Importantly, we uncovered that FTO operates a regulatory network of m^{6}A modification that involves METTL14, YTHDF1 and AKT3 signaling, providing the first insight into the mechanism of FTO-mediated esophageal cancer progression.

Materials And Methods

Samples, cell lines, and plasmids

The 28 human esophageal cancer samples were obtained from abdominal surgery at the First Affiliated Hospital of University of Science and Technology of China, and patients provided informed consent. The pathological condition was determined by an experienced surgical specialist. The comprehensive clinical and pathological information of esophageal cancer patients is shown in SI Appendix, Table S1. The esophageal cancer cell lines KYSE140, KYSE180, KYSE450, KYSE30,and KYSE150 and the human normal esophageal epithelial cell line HEEC were obtained from the Chinese Academy of Cell Resource Center (Shanghai, China) [61].

Lentiviruses for overexpressing and silencing the expression of FTO, METTL14 and AKT3 were constructed from Hanbio Biotechnology Co., Ltd. Plasmids for the expression of Flag-tagged wild-type

(YTHDF1-WT, YTHDF2-WT, YTHDF3-WT, YTHDC1-WT, YTHDC2-WT) were constructed withthep3xFLAG-*Myc*-CMV vector. Detailed information regarding the primers used for plasmid construction is depicted in SI Appendix, Table S2. For shRNA plasmids used in lentivirus-mediated interference, complementary sense and antisense oligo nucleotides encoding shRNAs targeting YTHDF1 were synthesized, annealed and cloned into the pHBLV-U6-MCS-EF1-mcherry-T2A-PURO vector. The related sequences of shRNAs are shown in Table S2 of the SI Appendix.

Gene expression and survival analysis in esophageal cancer datasets

Kaplan–Meier plotter (http://kmplot.com/analysis/) was used to assess the prognostic value of FTO and METTL14 expression in patients with esophageal cancer. The mRNA expression of FTO, YTHDC1, and YTHDF1 in cancer tissues and matched adjacent normal tissues of esophageal cancer patients was obtained from TCGA (The Cancer Genome Atlas) database. GEPIA2 (http://gepia.cancer-pku.cn/) was used to assess the correlation analysis of FTO and AKT3.

m^{6}A content analysis

The EpiQuik TM m^{6}A RNA Methylation Quantification Kit (Epigentek) was used to analyze the content of m^{6}A in total RNA.

Dot blot assays

mRNA was obtained according to the PolyA Ttract® mRNA Isolation System (Promega) instruction manual. mRNA (50 ng/100 ng) was diluted to 2 μl with DEPC water and placed in a PCR instrument for thermal denaturation at 65 ℃ for 10 minutes. The denatured RNA was evenly dotted onto a positively charged nylon membrane (Beyotime). UV irradiation was placed under the operating platform for 15 minutes, and RNA was fixed to the membrane. The fixed nylon film was washed in 1 x PBST 3 times for 5 minutes each time. Ten milliliters of 5% skim milk sealant was prepared, and the membrane was placed in the sealant and sealed at room temperature for 2 hours. Rabbit m^{6}A primary antibody (active motif) was formulated at a ratio of 1:1000. The nylon membrane was dipped in the primary antibody and incubated overnight at 4 ℃. The nylon film incubated overnight was washed with PBST 3 times for 5 minutes each time. Rat anti-rabbit secondary antibody was prepared according to 1:2000. The nylon membrane was immersed in the secondary antibody and incubated at room temperature for 2 hours. The nylon film was washed 4 times with TBST for 5 minutes each time. The ECL color solution was prepared, and the nylon film was immersed in the color solution for 10 seconds. The nylon film was removed and observed under developer. Then, the nylon film was stained with 0.2% methylene blue dye (pH 5.2,

corrected by 0.3 M sodium acetate for pH) for 0.5 hours. Photographs were taken, and the sample load volume of each sample was compared.

The m^6ART–PCR

According to described protocol, m^6A-RT–PCR was conducted [62]. To obtain the m^6A pull-down portion, 2 μg RNA was used for immunoprecipitation with m^6A antibody in 500 μl IP buffer. m^6A RNA was immunoprecipitated with Dynabeads ® Protein A and then eluted twice with elution buffer. m^6A IP RNA was recovered by ethanol precipitation. Then, 2 ng of the total RNA and m^6A IP RNA were used as templates in qRT–PCR.

In vitro cell assays

Total of 5×10^3 cells per well were seeded onto a 96-well plate and checked every 24 hours (0, 24, 48, 72 and 96 hours), and cell proliferation was measured using CCK-8.

The cell migration test was performed in a 24-well plate with an 8 μm pore size Transwell chamber (Corning). A total of 200 μl of a suspension containing 5×10^4 cells made of RPMI 1640 without FBS was inoculated into the upper part of the chamber. Then,600 μl of RPMI 1640 medium containing 20% FBS was added to the lower part of the chamber. After incubation for 30 hours at 37 ℃ and 5% CO_2, the transwell chamber was removed, the culture medium in the well was discarded, the cells were washed twice with PBS, fixed with methanol for 5 minutes, stained with 0.1% crystal violet for 30 minutes, the upper layer of cells was wiped off with a cotton swab, and the cells were washed with PBS 3 times. Five fields of view were randomly taken under the microscope to observe the cells and count them.

Cell invasion assays were performed in a 24-well plate with 8 μm pore size chamber inserts (Corning). A total of 8×10^4 cells were seeded in the upper portion of the invasion chamber with 200 μl of RPMI 1640 without FBS. The lower portion of the chamber contained 600 μl of medium supplemented with 20% FBS and glutamine. After incubation for 36 hours at 37 ℃ and 5% CO_2, the noninvading cells were removed from the upper surface of the membrane. Cells that moved to the bottom surface of the chamber were stained with 0.1% crystal violet for 30 minutes. The cells were then imaged and counted in four separate areas with an inverted microscope.

RNA pull-down assays

RNA was taken from the Megascript® T7 Transcription Kit (Ambion) through the *in vitro* Transcription Kit, and then the Pierce Magnetic RNA-Protein Pull-Down Kit (Thermo Scientific) was used to conduct the RNA pull-down experiment. In short, a Pierce RNA 3' End Desthiobiotinylation Kit (Thermo Scientific) was used to biotin the RNA. Then, 50 pmol of biotinylated RNA, 50 μl of streptavidin magnetic beads and 200

μg of cell lysates were incubated at a suitable temperature for a certain period of time, and the supernatant was collected after repeated washing for real-time PCR and Western blotting analysis. Detailed information regarding the primers used for real-time PCR analysis is depicted in SI Appendix, Table S2.

RIP assays

A Magna RIP RNA-Binding Protein Immunoprecipitation Kit (Millipore) was used for RIP according to the instructions [63]. Briefly, approximately 2–4 × 10^7 KYSE150 cells were lysed before centrifugation, incubated with magnetic beads and coated with antibodies for 4 hours or overnight at 4 ℃. Then, the complexes were washed and incubated with proteinase K. Then, the samples were centrifuged and placed on a magnetic separator, and the supernatants were used to extract RNA with an RNA extraction kit (Bioline). Purified RNA was used for analysis. Detailed information regarding the primers used for PCR analysis is depicted in SI Appendix, Table S2.

m^{6}A-seq and data analysis

Total RNA was isolated from KYSE150 and KYSE30 FTO knockdown (sh-FTO) cells using TRIzol reagent (Tiangen). RNA fragmentation, m^{6}A-seq, and library preparation were performed according to the manufacturer's instructions [64]. An RNA Library Prep Kit (NEB, USA) was used for library preparation. The m^{6}A-seq data were analyzed according to the manufacturer's protocols.

Vector and m^{6}A mutation assays

The potential m^{6}A sites of full-length AKT3 transcripts were predicted using an online tool, SRAMP (http://www.cuilab.cn/sramp/). The m^{6}A motif-depleted 3'UTR regions were cloned into pGL3 for luciferase reporter gene analysis. The specific sequences are shown in SI Appendix, Table S2.

RNA stability

To measure the RNA stability of FTO knockdown in KYSE150 cells, actinomycete D (6 μg/ml)-treated control cells and down regulated FTO cells were used to block RNA transcription at 0, 2, 4, 6, and 8 hours. *AKT3* mRNA residue was detected by quantitative PCR, and the stability of mRNA was calculated.

Luciferase reporter assays

FTO knockdownKYSE150 cells were transfected with pGL3, pGL3-WT-3'UTR, pGL3-Mut1-3'UTR, or pGL3-Mut2-3'UTR in a 6-well plate. After transfection for 8 hours, each cell line was reseeded into a 96-well

plate. After 24 hours of incubation, both firefly and Renilla luciferase activities were measured 24 hours after transfection using the Dual-Luciferase Reporter Assay System (Promega) [65]. Detailed information regarding the primers used for plasmid construction is depicted in SI Appendix, Table S2.

In vivo xenograft model

For the subcutaneous transplanted model, sh-control, sh-FTO, NC-OE and AKT3-OE KYSE150 cells (6×10^6 per mouse, n = 3 for each group) were diluted in 100 μl of PBS + 100 μl Matrigel (BD) and subcutaneously injected into immuno deficient male mice to investigate tumor growth. When the tumor volume in each group reached ~100 mm^3, the mice were anesthetized with a small flow of carbon dioxide to make them unconscious. Then, the mice were killed completely by increasing the flow, and by pulling the leg of the mouse to see if there was muscle tension, the mice were judged as dead. Then, the tumors were removed and weighed for use in immunohistochemistry assays and further studies. The equation $V=0.5\times D\times d^2$ was used to calculate the tumor volume (V: volume, D: longitudinal diameter, d: latitudinal diameter). For the *in vivo* lung metastasis model, mice were injected with WT (wild-type), sh-FTO, AKT3-OE and sh-FTO+AKT3-OE KYSE150 cells (1×10^6 per mouse, n = 3 for each group). Six weeks after injection, mice were killed, and metastatic lung tumors were analyzed.

Immunohistochemistry assays

Tissue arrays were constructed using 28 pairs of esophageal cancer and paracancerous tissues as well as animal experimental specimens. Paraffin embedding, sectioning, and immunohistochemistry (IHC) were programmed to detect FTO expression in esophageal cancer and paracancerous tissues and Vimentin, E-cadherin, and MMP2 expression in animal specimens. Pictures were taken usinga LEICA DM 4000B microscope.

Statistical analysis

Microsoft Excel software and GraphPad Prism were used to assess the differences between experimental groups. Statistical significance was analyzed by a two-tailed Student's *t* test and one-way ANOVA. *p* values less than 0.05 were considered to be statistically significant: *, *p* value < 0.05; **, *p* value < 0.01; ***, *p* value < 0.001.

Abbreviations

m^6A: N^6-methyladenosine;

FTO: Fatmass and obesity-associated protein;

AKT3: AKT serine/threonine kinase 3;

METTL14: Methyltransferase-like 14;

WTAP: Wilms tumor 1 associated protein;

ALKBH5: alkylation repair homolog protein 5;

YTHDF1: YTH N^6-methyladenosine RNA binding protein 1;

YTHDF2: YTH N^6-methyladenosine RNA binding protein 2;

IGF2BP1: insulin-like growth factor 2 mRNA binding protein 1;

IGF2BP2: insulin-like growth factor 2 mRNA binding protein 2;

E-cad: E-cadherin;

VIM: Vimentin;

MMP2: Matrix metallopeptidase 2;

ActD: Actinomycetes D;

MeRIP-seq: Methylated RNA immunoprecipitation;

RNA-seq: Transcriptomic RNA sequencing;

IHC:Immunohistochemical;

RIP:RNA immunoprecipitation;

RT–qPCR: Quantitative real-time PCR;

SDS–PAGE: sodium dodecyl sulfate–polyacrylamide gel electrophoresis;

3'UTR: Three prime untranslated region;

CDS: coding sequence;

WT: wide-type;

PVDF: polyvinylidene fluoride;

TCGA: The Cancer Genome Atlas;

USTC: University of Science and Technology of China

Declarations

Ethics approval and consent to participate

The animal study proposal was approved by the Institutional Animal Care and Use Committee (IACUC) of the University of Science and Technology of China(2021-N(A)-139). All of the mouse experimental procedures were performed in accordance with the Regulations for the Administration of Affairs Concerning Experimental Animals approved by the State Council of People's Republic of China.

Consent for publication

Not applicable.

Availability of data and materials

Not applicable.

Competing interests

The authors declare that they have no competing interests.

Funding

This work was supported by the Anhui Provincial Natural Science Foundation of China (No. 2008085MH299). The Chen xiao-ping Foundation for the Development of Science and Technology of Hubei province (CXPIJHL2000005-07-34). The fundamental Research Funds for the Central Universities (WK9110000086). The Postdoctoral Research Funding of Anhui Province in 2019 (2019B371). The Youth Technical Backbone Fund of West Branch of the First Affiliated Hospital of USTC granted to CBZ and LSK, respectively.

Authors' contributions

RW and CBZ carried out the structure of the experiments and revised the manuscript; FFZ, YHL and CBZ drafted the initial manuscript; ZYL and LSK conceived of the study, participated in its design and coordination and helped draft the manuscript. All authors read and approved the final manuscript.

Acknowledgements

We thank Prof. YongLiang Jiang on proofreading the manuscript and the staff who participated in this study.

References

1. Meyer KD, Jaffrey SR: **Rethinking m(6)A Readers, Writers, and Erasers**. *Annual review of cell and developmental biology* 2017, **33**:319-342.

2. Balacco DL, Soller M: **The m(6)A Writer: Rise of a Machine for Growing Tasks**. *Biochemistry* 2019, **58**(5):363-378.
3. Holzer H: **Chemistry and biology of macromolecular inhibitors from yeast acting on proteinases A and B, and carboxypeptidase Y**. *Advances in enzyme regulation* 1975, **13**:125-134.
4. Sadecky E, Brezina R, Kazar J, Urvolgyi J: **Immunization against Q-fever of naturally infected dairy cows**. *Acta virologica* 1975, **19**(6):486-488.
5. Poole-Wilson PA, Langer GA: **Effect of pH on ionic exchange and function in rat and rabbit myocardium**. *The American journal of physiology* 1975, **229**(3):570-581.
6. Jia G, Fu Y, Zhao X, Dai Q, Zheng G, Yang Y, Yi C, Lindahl T, Pan T, Yang YG *et al*: **N6-methyladenosine in nuclear RNA is a major substrate of the obesity-associated FTO**. *Nature chemical biology* 2011, **7**(12):885-887.
7. Bland RD, Clarke TL, Harden LB: **Rapid infusion of sodium bicarbonate and albumin into high-risk premature infants soon after birth: a controlled, prospective trial**. *American journal of obstetrics and gynecology* 1976, **124**(3):263-267.
8. Zhao BS, Wang X, Beadell AV, Lu Z, Shi H, Kuuspalu A, Ho RK, He C: **m(6)A-dependent maternal mRNA clearance facilitates zebrafish maternal-to-zygotic transition**. *Nature* 2017, **542**(7642):475-478.
9. Wang X, Lu Z, Gomez A, Hon GC, Yue Y, Han D, Fu Y, Parisien M, Dai Q, Jia G *et al*: **N6-methyladenosine-dependent regulation of messenger RNA stability**. *Nature* 2014, **505**(7481):117-120.
10. Wang X, Zhao BS, Roundtree IA, Lu Z, Han D, Ma H, Weng X, Chen K, Shi H, He C: **N(6)-methyladenosine Modulates Messenger RNA Translation Efficiency**. *Cell* 2015, **161**(6):1388-1399.
11. Fu Y, Luo GZ, Chen K, Deng X, Yu M, Han D, Hao Z, Liu J, Lu X, Dore LC *et al*: **N6-methyldeoxyadenosine marks active transcription start sites in Chlamydomonas**. *Cell* 2015, **161**(4):879-892.
12. Zhang G, Huang H, Liu D, Cheng Y, Liu X, Zhang W, Yin R, Zhang D, Zhang P, Liu J *et al*: **N6-methyladenine DNA modification in Drosophila**. *Cell* 2015, **161**(4):893-906.
13. Zhou J, Wan J, Gao X, Zhang X, Jaffrey SR, Qian SB: **Dynamic m(6)A mRNA methylation directs translational control of heat shock response**. *Nature* 2015, **526**(7574):591-594.
14. Roundtree IA, Evans ME, Pan T, He C: **Dynamic RNA Modifications in Gene Expression Regulation**. *Cell* 2017, **169**(7):1187-1200.
15. Yue Y, Liu J, He C: **RNA N6-methyladenosine methylation in post-transcriptional gene expression regulation**. *Genes & development* 2015, **29**(13):1343-1355.
16. Xiang Y, Laurent B, Hsu CH, Nachtergaele S, Lu Z, Sheng W, Xu C, Chen H, Ouyang J, Wang S *et al*: **Corrigendum: RNA m(6)A methylation regulates the ultraviolet-induced DNA damage response**. *Nature* 2017, **552**(7685):430.

17. Xiang Y, Laurent B, Hsu CH, Nachtergaele S, Lu Z, Sheng W, Xu C, Chen H, Ouyang J, Wang S *et al*: **RNA m(6)A methylation regulates the ultraviolet-induced DNA damage response**. *Nature* 2017, **543**(7646):573-576.
18. Lence T, Akhtar J, Bayer M, Schmid K, Spindler L, Ho CH, Kreim N, Andrade-Navarro MA, Poeck B, Helm M *et al*: **m(6)A modulates neuronal functions and sex determination in Drosophila**. *Nature* 2016, **540**(7632):242-247.
19. Yoon KJ, Ringeling FR, Vissers C, Jacob F, Pokrass M, Jimenez-Cyrus D, Su Y, Kim NS, Zhu Y, Zheng L *et al*: **Temporal Control of Mammalian Cortical Neurogenesis by m(6)A Methylation**. *Cell* 2017, **171**(4):877-889 e817.
20. Zhang C, Chen Y, Sun B, Wang L, Yang Y, Ma D, Lv J, Heng J, Ding Y, Xue Y *et al*: **m(6)A modulates haematopoietic stem and progenitor cell specification**. *Nature* 2017, **549**(7671):273-276.
21. Li HB, Tong J, Zhu S, Batista PJ, Duffy EE, Zhao J, Bailis W, Cao G, Kroehling L, Chen Y *et al*: **m(6)A mRNA methylation controls T cell homeostasis by targeting the IL-7/STAT5/SOCS pathways**. *Nature* 2017, **548**(7667):338-342.
22. !!! INVALID CITATION !!!
23. Fischer J, Koch L, Emmerling C, Vierkotten J, Peters T, Bruning JC, Ruther U: **Inactivation of the Fto gene protects from obesity**. *Nature* 2009, **458**(7240):894-898.
24. Church C, Moir L, McMurray F, Girard C, Banks GT, Teboul L, Wells S, Bruning JC, Nolan PM, Ashcroft FM *et al*: **Overexpression of Fto leads to increased food intake and results in obesity**. *Nature genetics* 2010, **42**(12):1086-1092.
25. Merkestein M, Laber S, McMurray F, Andrew D, Sachse G, Sanderson J, Li M, Usher S, Sellayah D, Ashcroft FM *et al*: **FTO influences adipogenesis by regulating mitotic clonal expansion**. *Nature communications* 2015, **6**:6792.
26. Soderberg KC, Kaprio J, Verkasalo PK, Pukkala E, Koskenvuo M, Lundqvist E, Feychting M: **Overweight, obesity and risk of haematological malignancies: a cohort study of Swedish and Finnish twins**. *Eur J Cancer* 2009, **45**(7):1232-1238.
27. Li G, Chen Q, Wang L, Ke D, Yuan Z: **Association between FTO gene polymorphism and cancer risk: evidence from 16,277 cases and 31,153 controls**. *Tumour biology : the journal of the International Society for Oncodevelopmental Biology and Medicine* 2012, **33**(4):1237-1243.
28. Hernandez-Caballero ME, Sierra-Ramirez JA: **Single nucleotide polymorphisms of the FTO gene and cancer risk: an overview**. *Molecular biology reports* 2015, **42**(3):699-704.
29. Liu S, Huang M, Chen Z, Chen J, Chao Q, Yin X, Quan M: **FTO promotes cell proliferation and migration in esophageal squamous cell carcinoma through up-regulation of MMP13**. *Experimental cell research* 2020, **389**(1):111894.
30. Niu Y, Lin Z, Wan A, Chen H, Liang H, Sun L, Wang Y, Li X, Xiong XF, Wei B *et al*: **RNA N6-methyladenosine demethylase FTO promotes breast tumor progression through inhibiting BNIP3**. *Molecular cancer* 2019, **18**(1):46.

31. Guimaraes-Teixeira C, Barros-Silva D, Lobo J, Soares-Fernandes D, Constancio V, Leite-Silva P, Silva-Santos R, Braga I, Henrique R, Miranda-Goncalves V *et al*: **Deregulation of N6-Methyladenosine RNA Modification and Its Erasers FTO/ALKBH5 among the Main Renal Cell Tumor Subtypes**. *Journal of personalized medicine* 2021, **11**(10).
32. Li Z, Weng H, Su R, Weng X, Zuo Z, Li C, Huang H, Nachtergaele S, Dong L, Hu C *et al*: **FTO Plays an Oncogenic Role in Acute Myeloid Leukemia as a N(6)-Methyladenosine RNA Demethylase**. *Cancer cell* 2017, **31**(1):127-141.
33. Kato H, Nakajima M: **Treatments for esophageal cancer: a review**. *General thoracic and cardiovascular surgery* 2013, **61**(6):330-335.
34. Xu QL, Li H, Zhu YJ, Xu G: **The treatments and postoperative complications of esophageal cancer: a review**. *Journal of cardiothoracic surgery* 2020, **15**(1):163.
35. Lin X, Chai G, Wu Y, Li J, Chen F, Liu J, Luo G, Tauler J, Du J, Lin S *et al*: **RNA m(6)A methylation regulates the epithelial mesenchymal transition of cancer cells and translation of Snail**. *Nature communications* 2019, **10**(1):2065.
36. Petrova YI, Schecterson L, Gumbiner BM: **Roles for E-cadherin cell surface regulation in cancer**. *Molecular biology of the cell* 2016, **27**(21):3233-3244.
37. Yang X, Zhang S, He C, Xue P, Zhang L, He Z, Zang L, Feng B, Sun J, Zheng M: **METTL14 suppresses proliferation and metastasis of colorectal cancer by down-regulating oncogenic long non-coding RNA XIST**. *Molecular cancer* 2020, **19**(1):46.
38. Weng H, Huang H, Wu H, Qin X, Zhao BS, Dong L, Shi H, Skibbe J, Shen C, Hu C *et al*: **METTL14 Inhibits Hematopoietic Stem/Progenitor Differentiation and Promotes Leukemogenesis via mRNA m(6)A Modification**. *Cell stem cell* 2018, **22**(2):191-205 e199.
39. Lan Q, Liu PY, Haase J, Bell JL, Huttelmaier S, Liu T: **The Critical Role of RNA m(6)A Methylation in Cancer**. *Cancer research* 2019, **79**(7):1285-1292.
40. Chen XY, Zhang J, Zhu JS: **The role of m(6)A RNA methylation in human cancer**. *Molecular cancer* 2019, **18**(1):103.
41. Hinz N, Jucker M: **Distinct functions of AKT isoforms in breast cancer: a comprehensive review**. *Cell communication and signaling : CCS* 2019, **17**(1):154.
42. Toulany M, Maier J, Iida M, Rebholz S, Holler M, Grottke A, Juker M, Wheeler DL, Rothbauer U, Rodemann HP: **Akt1 and Akt3 but not Akt2 through interaction with DNA-PKcs stimulate proliferation and post-irradiation cell survival of K-RAS-mutated cancer cells**. *Cell death discovery* 2017, **3**:17072.
43. Liu Q, Qu X, Xie X, He P, Huang S: **Repression of Akt3 gene transcription by the tumor suppressor RIZ1**. *Scientific reports* 2018, **8**(1):1528.
44. Dashti Y, Grkovic T, Abdelmohsen UR, Hentschel U, Quinn RJ: **Actinomycete Metabolome Induction/Suppression with N-Acetylglucosamine**. *Journal of natural products* 2017, **80**(4):828-836.
45. Silen W, Machen TE, Forte JG: **Acid-base balance in amphibian gastric mucosa**. *The American journal of physiology* 1975, **229**(3):721-730.

46. Kidder GW, Montgomery CW: **Oxygenation of frog gastric mucosa in vitro**. *The American journal of physiology* 1975, **229**(6):1510-1513.
47. Cui Q, Shi H, Ye P, Li L, Qu Q, Sun G, Lu Z, Huang Y, Yang CG, Riggs AD *et al*: **m(6)A RNA Methylation Regulates the Self-Renewal and Tumorigenesis of Glioblastoma Stem Cells**. *Cell reports* 2017, **18**(11):2622-2634.
48. Altomare DA, Testa JR: **Perturbations of the AKT signaling pathway in human cancer**. *Oncogene* 2005, **24**(50):7455-7464.
49. Castaneda CA, Cortes-Funes H, Gomez HL, Ciruelos EM: **The phosphatidyl inositol 3-kinase/AKT signaling pathway in breast cancer**. *Cancer metastasis reviews* 2010, **29**(4):751-759.
50. Nicholson KM, Anderson NG: **The protein kinase B/Akt signalling pathway in human malignancy**. *Cellular signalling* 2002, **14**(5):381-395.
51. Barnett SF, Defeo-Jones D, Fu S, Hancock PJ, Haskell KM, Jones RE, Kahana JA, Kral AM, Leander K, Lee LL *et al*: **Identification and characterization of pleckstrin-homology-domain-dependent and isoenzyme-specific Akt inhibitors**. *The Biochemical journal* 2005, **385**(Pt 2):399-408.
52. Hernandez-Aya LF, Gonzalez-Angulo AM: **Targeting the phosphatidylinositol 3-kinase signaling pathway in breast cancer**. *The oncologist* 2011, **16**(4):404-414.
53. Araki K, Miyoshi Y: **Mechanism of resistance to endocrine therapy in breast cancer: the important role of PI3K/Akt/mTOR in estrogen receptor-positive, HER2-negative breast cancer**. *Breast Cancer* 2018, **25**(4):392-401.
54. Lopez-Knowles E, O'Toole SA, McNeil CM, Millar EK, Qiu MR, Crea P, Daly RJ, Musgrove EA, Sutherland RL: **PI3K pathway activation in breast cancer is associated with the basal-like phenotype and cancer-specific mortality**. *International journal of cancer* 2010, **126**(5):1121-1131.
55. Ma JZ, Yang F, Zhou CC, Liu F, Yuan JH, Wang F, Wang TT, Xu QG, Zhou WP, Sun SH: **METTL14 suppresses the metastatic potential of hepatocellular carcinoma by modulating N(6) -methyladenosine-dependent primary MicroRNA processing**. *Hepatology* 2017, **65**(2):529-543.
56. Zhao BS, Roundtree IA, He C: **Post-transcriptional gene regulation by mRNA modifications**. *Nature reviews Molecular cell biology* 2017, **18**(1):31-42.
57. Zhao BS, Roundtree IA, He C: **Publisher Correction: Post-transcriptional gene regulation by mRNA modifications**. *Nature reviews Molecular cell biology* 2018, **19**(12):808.
58. Shi Y, Fan S, Wu M, Zuo Z, Li X, Jiang L, Shen Q, Xu P, Zeng L, Zhou Y *et al*: **YTHDF1 links hypoxia adaptation and non-small cell lung cancer progression**. *Nature communications* 2019, **10**(1):4892.
59. Bai Y, Yang C, Wu R, Huang L, Song S, Li W, Yan P, Lin C, Li D, Zhang Y: **YTHDF1 Regulates Tumorigenicity and Cancer Stem Cell-Like Activity in Human Colorectal Carcinoma**. *Frontiers in oncology* 2019, **9**:332.
60. Liu T, Wei Q, Jin J, Luo Q, Liu Y, Yang Y, Cheng C, Li L, Pi J, Si Y *et al*: **The m6A reader YTHDF1 promotes ovarian cancer progression via augmenting EIF3C translation**. *Nucleic acids research* 2020, **48**(7):3816-3831.

61. Zang C, Zhao F, Pu Y: **LMX1B involved in the radioresistance, proliferation and migration of esophageal cancer cells**. *Biomedicine & pharmacotherapy = Biomedecine & pharmacotherapie* 2019, **118**:109358.
62. Cheng M, Sheng L, Gao Q, Xiong Q, Zhang H, Wu M, Liang Y, Zhu F, Zhang Y, Zhang X *et al*: **The m(6)A methyltransferase METTL3 promotes bladder cancer progression via AFF4/NF-kappaB/MYC signaling network**. *Oncogene* 2019, **38**(19):3667-3680.
63. Sang B, Zhang YY, Guo ST, Kong LF, Cheng Q, Liu GZ, Thorne RF, Zhang XD, Jin L, Wu M: **Dual functions for OVAAL in initiation of RAF/MEK/ERK prosurvival signals and evasion of p27-mediated cellular senescence**. *Proceedings of the National Academy of Sciences of the United States of America* 2018, **115**(50):E11661-E11670.
64. Ping XL, Sun BF, Wang L, Xiao W, Yang X, Wang WJ, Adhikari S, Shi Y, Lv Y, Chen YS *et al*: **Mammalian WTAP is a regulatory subunit of the RNA N6-methyladenosine methyltransferase**. *Cell research* 2014, **24**(2):177-189.
65. Pu Y, Zhao F, Wang H, Cai W, Gao J, Li Y, Cai S: **Correction: MiR-34a-5p promotes the multi-drug resistance of osteosarcoma by targeting the CD117 gene**. *Oncotarget* 2017, **8**(36):60723.

Figures

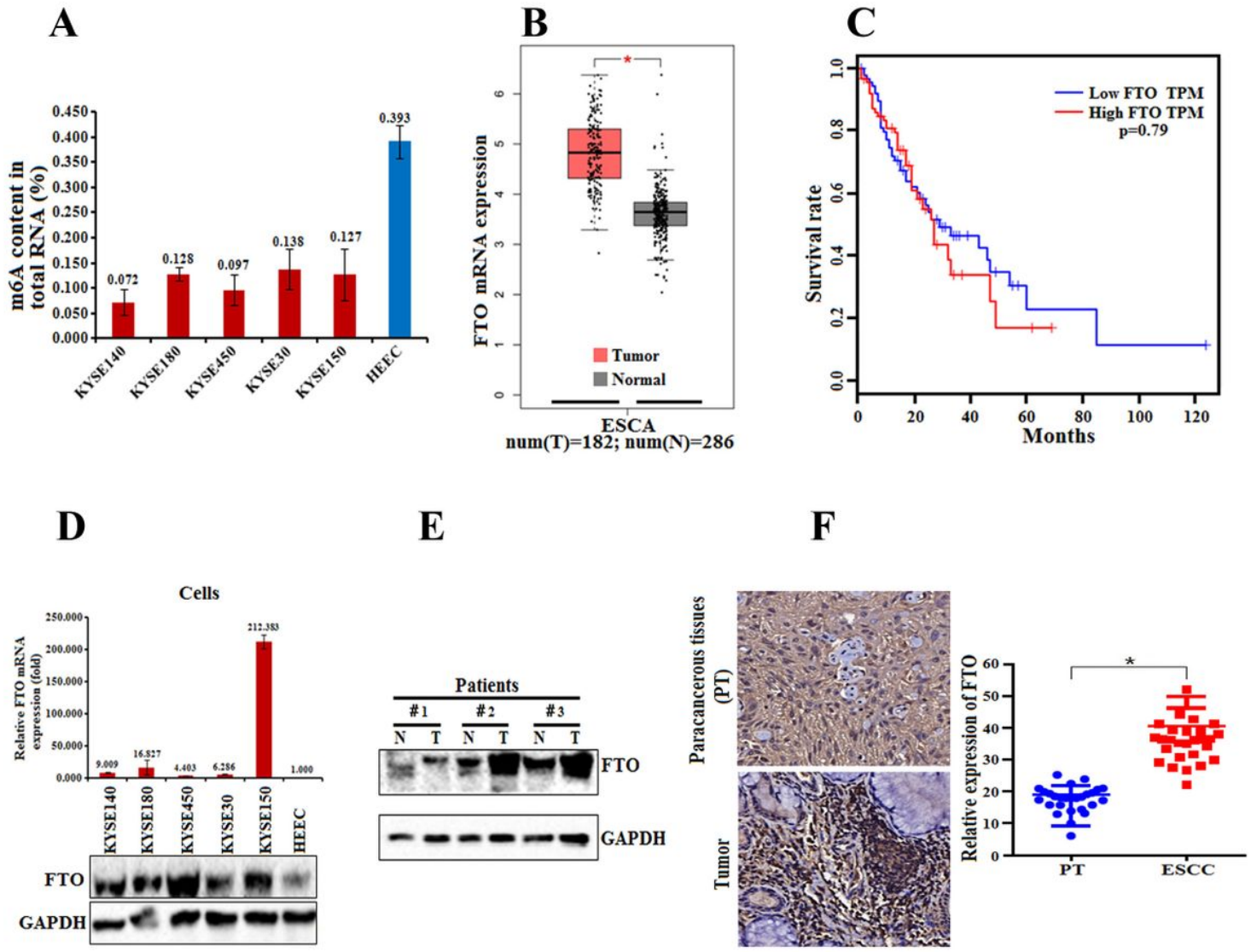

Figure 1

FTO expression in normal esophageal tissue and esophageal cancer patients.

A.mRNA m^{6}A level in five esophageal cancer cell lines and one normal esophageal cell line (HEEC) determined by MeRIP-PCR with m^{6}A RNA Methylation Quantification ELISA kit.

B.FTO was up-regulated inesophageal cancer patients compared with normal tissues (GEPIA data, Red box for tumor tissue, n = 182; gray box for normal tissue, n = 286).

C.Kaplan–Meier survival analysis of patient overall survival according to FTO levels in esophageal cancer tissues. n = 182, High FTO = 91, Low FTO = 91, *p* value is 0.79.

D.Real-time PCR analysis and western blotting assay of FTO expression in five esophageal cancer cell lines and one normal esophageal cell line.

E.Western blotting assay of FTO expression in three paired esophageal cancer primary tumor samples.

F. Representative image of immunohistochemical staining by FTO in 400 fold magnified ESCC tissues and paired normal tissues in human samples (above).Immunohistochemical expression of FTO in ESCC tumor tissue and paired paracancerous tissues (PT) was quantitatively analyzed using IMAGE-PRO PLUS 6.0 software (below). Scale bar 50 μm, n = 28.

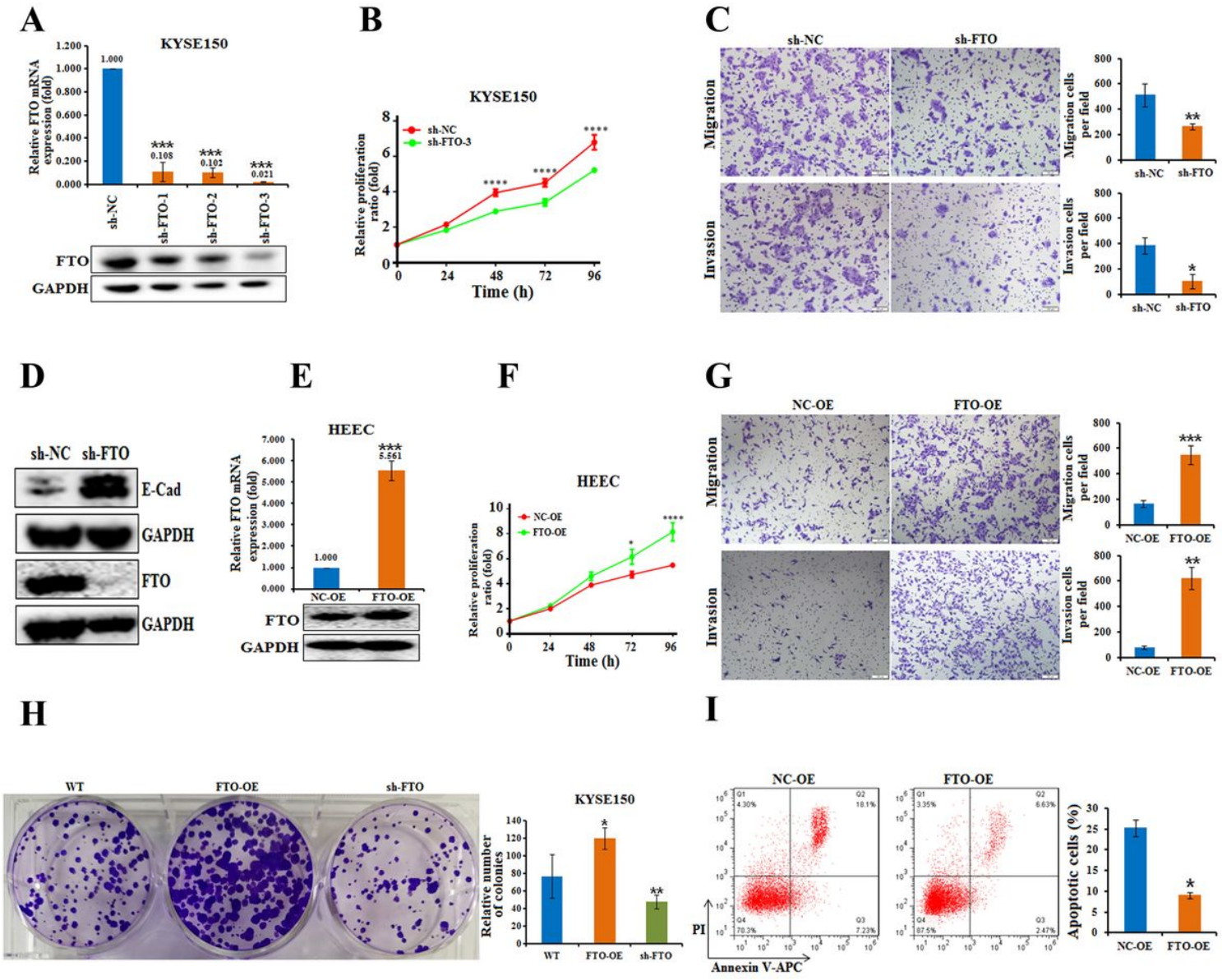

Figure 2

Effect of FTO on Esophageal cancer cells proliferation, migration, invasion, apoptosis and colonies.

A.The knockdown effect of specific shRNAs (sh-FTO-1, -2 and -3) in KYSE150 cells was verified at both the mRNA (by qRT-PCR) and protein levels (by western blot). ***,*p* value < 0.001.

B.CCK-8 assays every 24 hours showed that FTO knockdown inhibited the proliferation of KYSE150 cells versus the negative control (sh-NC). ***, *p* value < 0.001.

C.FTO knockdown in KYSE150 cells decreased migration and invasion compared to that of the negative control (sh-NC). The invasive ability of the cells was assessed by Image-Pro Plus 6.0 software. *, *p* value < 0.05; **, *p* value < 0.01.

D.The protein levels of E-cadherin and FTO in KYSE150 cells with FTO knockdown versus the negative control (sh-NC) measured by western blot analyses.

E.The levels of FTO in HEEC cells transfected with FTO-OE versus the negative control (NC-OE) measured by real-time PCR and western blot analyses are shown. n.s, no statistical significance; *, *p* value < 0.05; **, *p* value < 0.01.

F.CCK-8 assays every 24 hours showed that FTO overexpression promoted the proliferation of HEEC cells versus the negative control (NC-OE). n.s, no statistical significance; *, *p* value < 0.05;***,*p* value < 0.001.

G.FTO overexpression in HEEC cells increased migration and invasion compared to that of the negative control (NC-OE). The invasive ability of the cells was assessed by Image-Pro Plus 6.0 software. **,*p* value < 0.01; ***, *p*value < 0.001.

H.Colony formation assays showed that FTOpromoted cell proliferation in KYSE150 cells treated with FTO-expressing lentivirus (FTO-OE) and FTO knockdown (sh-FTO)versus the wide type (WT).

I.FTO overexpression in HEEC cells decreased apoptosis in Annexin V/PI staining analyzed by FACS. Quantification of apoptotic cells were plotted, numbers represent the sum of early and late apoptotic cells.

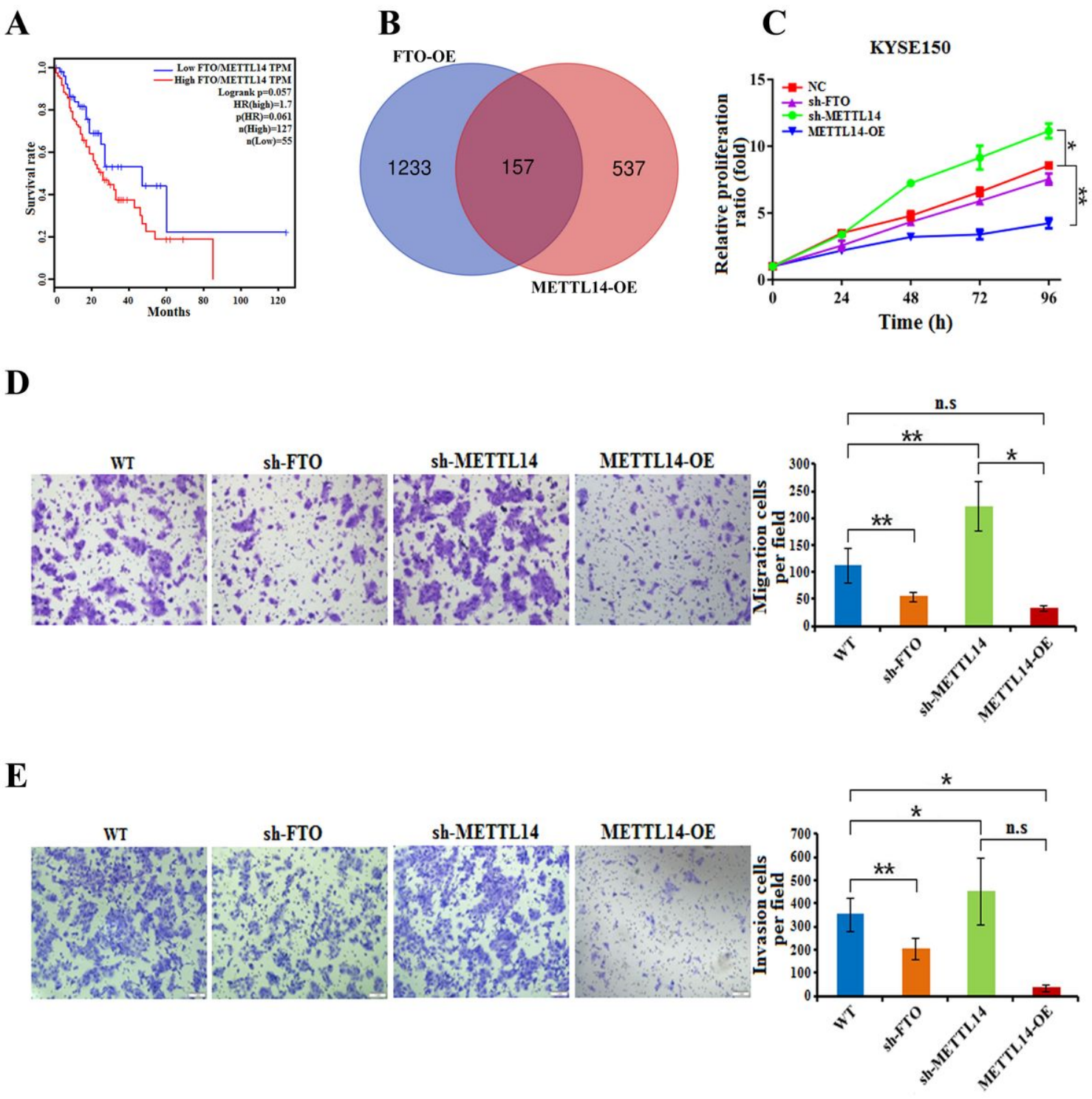

Figure 3

Correlation analysis of FTO and METTL14.

A.Kaplan–Meier survival analysis of patient overall survival according to the ratio of FTO mRNA expression to METTL14 expression levels in esophageal cancer tissues, the higher of the ratio, the worse the prognosis. High =127, Low FTO=55, *p* value is 0.057.

B.Wayne diagram analysis shows that the intersection genes overexpression FTO (FTO-OE) in KYSE150 and overexpression METTL14 (METTL14-OE) in KYSE150 cells.

C.CCK-8 assays every 24 hours showed that FTO knockdown inhibited the proliferation of KYSE150 cells, while METTL14 knockdown (sh-METTL14) or overexpression (METTL14-OE) can inhibit or restore FTO function.

D.FTO knockdown in KYSE150 cells decreased migration, while METTL14 knockdown (sh-METTL14) or overexpression (METTL14-OE) can inhibit or restore FTO function. The migrative ability of the cells was assessed by Image-Pro Plus 6.0 software. n.s, no statistical significance; *, *p* value < 0.05; **, *p* value < 0.01.

E.FTO knockdown in KYSE150 cells decreased invasion, while METTL14 knockdown (sh-METTL14) or overexpression (METTL14-OE) can inhibit or restore FTO function. The invasive ability of the cells was assessed by Image-Pro Plus 6.0 software. n.s, no statistical significance; *, *p* value < 0.05; **, *p* value < 0.01.

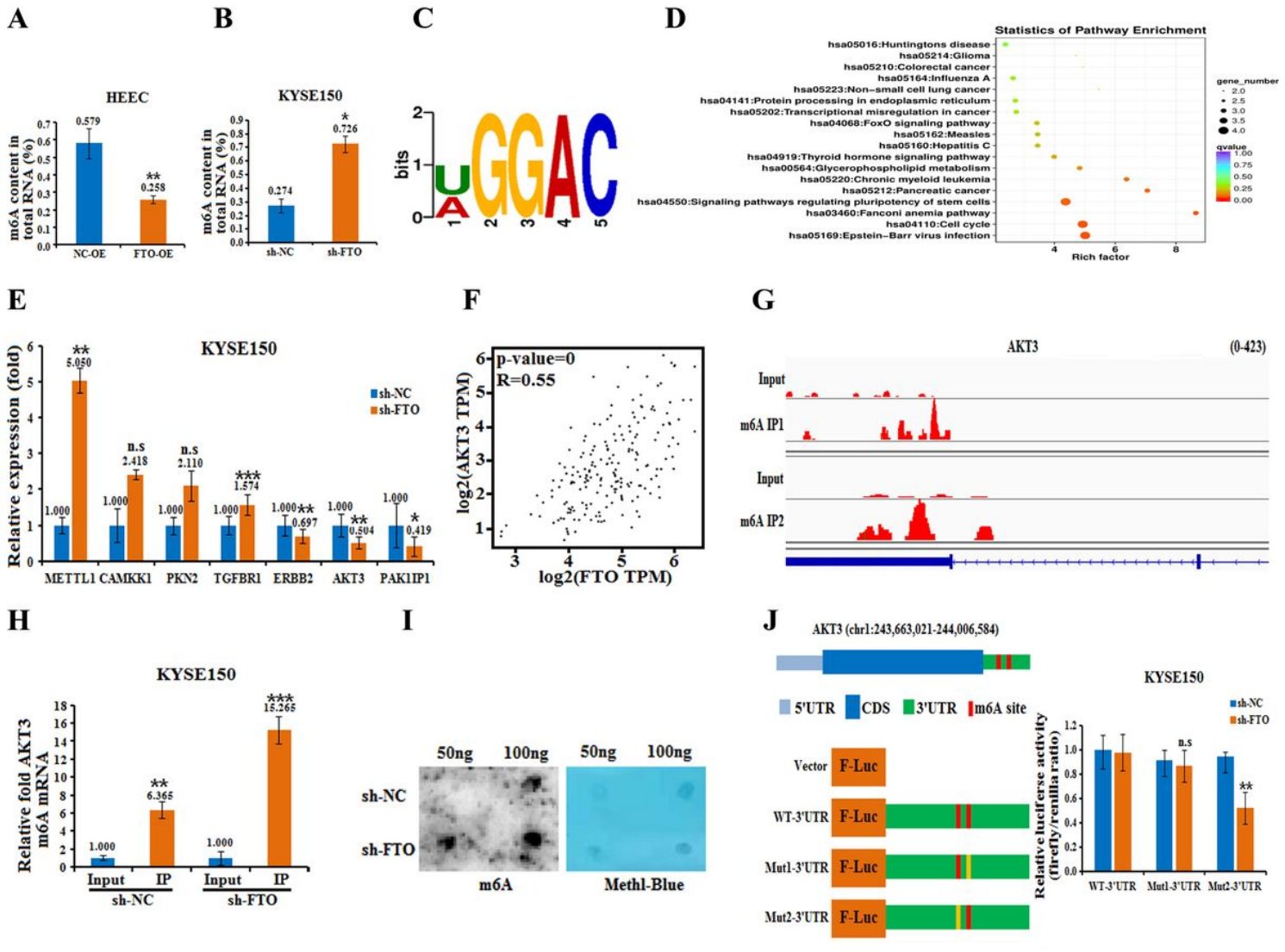

Figure 4

Identification of potential targets of FTO in esophageal cancer cells via transcriptome-wide m^{6}A-seq and RNA-Seq assays.

A and B.HEEC and KYSE150 cells were treated with FTO overexpression (FTO-OE) (**A**) or knockdown (sh-FTO)(**B**), the m^{6}A content of the total mRNA were determined with m^{6}A RNA Methylation Quantification Kit.

C.The motif of FTO was analyzed by the RMBase V2.0 database (http://rna.sysu.edu.cn/rmbase/).

D.A cluster profiler identified the enriched KEGG processes of 128 genes, which showed 1.5-fold m^{6}A expression upregulation in esophageal cancer cells compared with control cells.

E.The mRNA level of six differential genes *METTL1*, *CAMKK1*, *PKN2*, *TGFBR1*, *ERBB2*, *AKT3* and *PAK1P1* in KYSE150 cells with FTO knockdown versus the negative control (sh-NC) measured by real-time PCR. n.s, no statistical significance; *, *p* value < 0.05; **, *p* value < 0.01; ***,*p* value < 0.001.

F.The interaction of *FTO* and *AKT3* genes was analyzed using the GEPIA database.

G.The m^{6}A abundances on *AKT3* mRNA transcripts in KYSE30 and KYSE150 cells as detected by m^{6}A-seq are plotted using Integrative genomics viewer (IGV). The y axis shows sequence read number, blue boxes represent exons, and blue lines represent introns. Reduction of m^{6}A modification in specific regions of *AKT3*.

H.Detection of m^{6}A methylation levels in *AKT3* by MeRIP-PCR with m^{6}A RNA Methylation Quantification ELISA kit.

I. Dot plot analysis of the overall level of m^{6}A modification in esophageal cancer cells before and after knockdown of FTO m^{6}A modification site.

J.Schematic representation of positions of m^{6}A motifs within *AKT3* mRNA and the 3'UTR mutation (GGAC to GGCC) of pmirGLO vector to investigate the m^{6}A roles on *AKT3* expression. pmirGLO-WT-3'UTR or pmirGLO-Mut1/2-3'UTR reporters were transfected into KYSE150 cells with FTO knockdown versus the negative control (sh-NC), then the relative luciferase activity was measured.

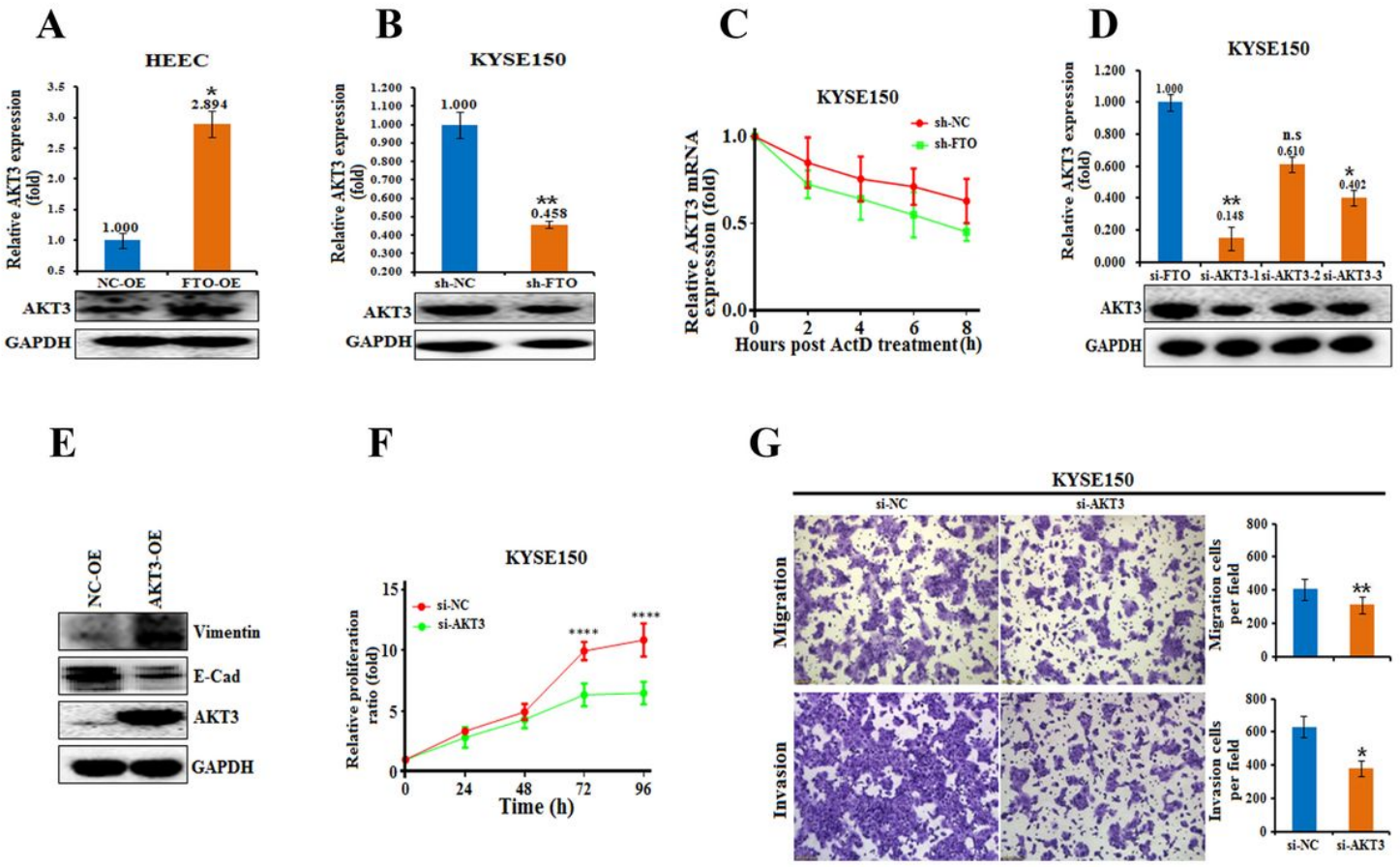

Figure 5

AKT3 is a critical target of FTO that mediate esophageal cancer cells growth, survival, and invasion

A.The levels of *AKT3* in HEEC cells transfected with FTO-OE versus the negative control (NC-OE) measured by real-time PCR and western blot analyses are shown. *, *p* value < 0.05.

B.The levels of *AKT3* in KYSE150 cells with FTO knockdown versus the negative control (sh-NC) measured by real-time PCR and western blot analyses are shown. **, *p* value < 0.01.

C.The mRNA level of *AKT3* in KYSE150 cells with FTO knockdown and then treated with Actinomycete D (6μg/ml) in 0, 2, 4, 6, 8 hours measured by real-time PCR.

D.The knockdown effect of specific siRNAs (si-*AKT3*-1, -2 and -3) in KYSE150 cells was verified at both the mRNA (by qRT-PCR) and protein levels (by western blot). n.s, no statistical significance; *, *p* value < 0.05; **, *p* value < 0.01.

E.The protein levels of Vimentin and AKT3 in KYSE150 cells with AKT3 overexpression versus the negative control (NC-OE) measured by western blot analyses.

F.CCK-8 assays every 24 hours showed that AKT3 knockdown inhibited the proliferation of KYSE150 cells versus the negative control (sh-NC). ***, *p* value < 0.001.

G.AKT3 knockdown in KYSE150 cells decreased migration and invasion compared to that of the negative control (si-NC). The invasive ability of the cells was assessed by Image-Pro Plus 6.0 software. *, *p* value < 0.05; **, *p* value < 0.01.

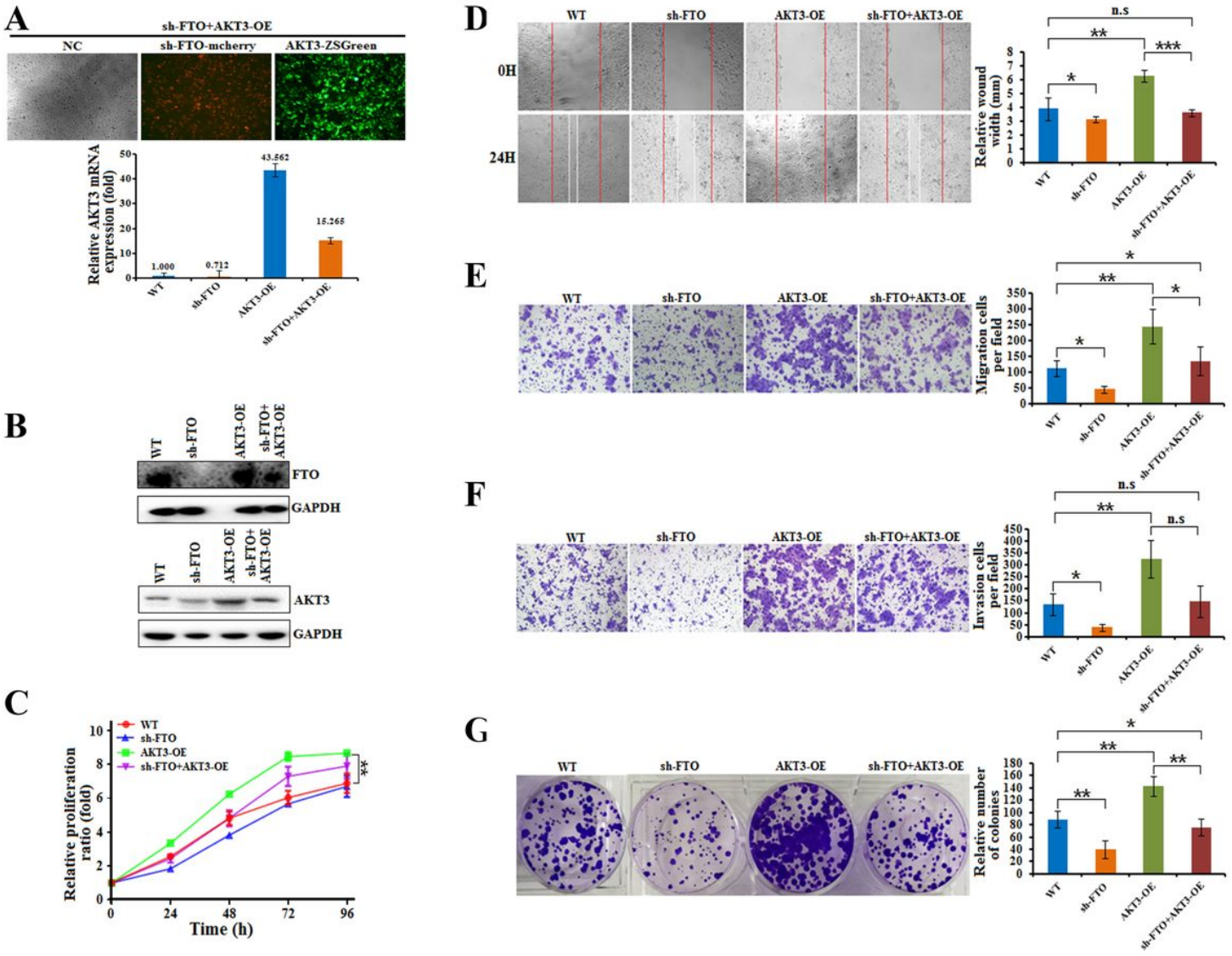

Figure 6

The functions of FTO and AKT3 on Esophageal cancer cells are mutually restricted

A.The relative AKT3 mRNA expression level in KYSE150 cells with FTO knockdown lentivirus (sh-FTO, mcherry), AKT3 expressing lentivirus (AKT3-OE, ZSGreen) and FTO knockdown adds AKT3 expressing lentivirus (sh-FTO+AKT3-OE) measured by qRT-PCR analyses.

B.The protein levels of FTO and AKT3 in KYSE150 cells with FTO knockdown lentivirus (sh-FTO), FTO knockdown adds AKT3 expressing lentivirus (sh-FTO+AKT3-OE) and AKT3 expressing lentivirus (AKT3-OE) measured by western blot analyses.

C.CCK-8 assays every 24 hours showed that FTO knockdown (sh-FTO) inhibited the proliferation of KYSE150 cells, while AKT3 overexpression (AKT3-OE) or FTO knockdown adds AKT3 overexpression (sh-FTO+AKT3-OE) can restore FTO function.

D.The wound healing of KYSE150 cells with FTO knockdown lentivirus (sh-FTO), AKT3 expressing lentivirus (AKT3-OE) and FTO knockdown adds AKT3 expressing lentivirus (sh-FTO+AKT3-OE) for 48h were recorded (left) and quantitatively analyzed (right).

E.FTO knockdown in KYSE150 cells decreased migration compared to that of the negative control (sh-NC), while AKT3 overexpression (AKT3-OE) or FTO knockdown adds AKT3 overexpression (sh-FTO+AKT3-OE) can restore FTO function.

F.FTO knockdown in KYSE150 cells decreased invasion compared to that of the negative control (sh-NC), while AKT3 overexpression (AKT3-OE) or FTO knockdown adds AKT3 overexpression (sh-FTO+AKT3-OE) can restore FTO function.

G.FTO knockdown in KYSE150 cells decreased colony formation compared to that of the negative control (sh-NC), while AKT3 overexpression (AKT3-OE) or FTO knockdown adds AKT3 overexpression (sh-FTO+AKT3-OE) can restore FTO function.

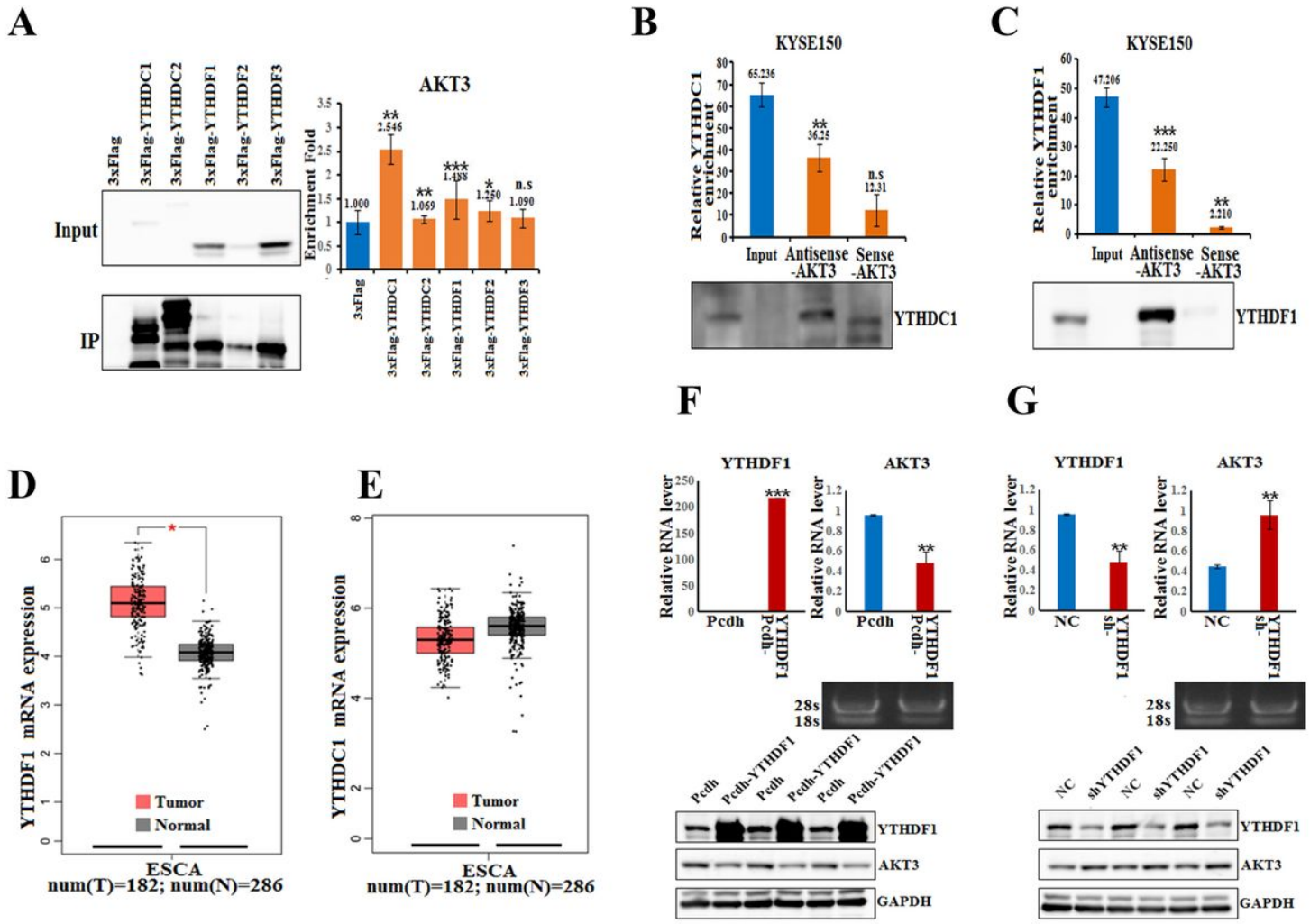

Figure 7

Binding verification of AKT3 gene with m^{6}A reader

A.RIP assays in KYSE150 cells using 3xFlag, 3xFlag-YTHDC1, 3xFlag-YTHDC2, 3xFlag-YTHDF1, 3xFlag-YTHDF2 and 3xFlag-YTHDF3 plasmid and Anti-Flag antibody. The western blots analyzed in the left showed that AKT3 interacts with YTHDC1 and YTHDF1 in KYSE150 cells. The expression of AKT3 analyzed by real-time PCR results of RIP assays are shown in the right top. n.s, no statistical significance; *, *p* value < 0.05;**, *p* value < 0.01; ***, *p*value < 0.001.

B.Pull down assays in KYSE150 cells were transfected with biotinylated AKT3 sense probe and antisense probe (50 μl streptavidin beads were washed once with RPD buffer, then 10 μl of sense robe and 10 μl of antisense probe were added, and incubated for overnight at 4 °C). Then cells were collected for the biotin-based pull-down assay. YTHDC1 expression levels were analyzed by real-time PCR analysis and western blotting. n.s, no statistical significance; **, p value < 0.01.

C.Pull down assays in KYSE150 cells were transfected with biotinylated AKT3 sense probe and antisense probe (50 μl streptavidin beads were washed once with RPD buffer, then 10 μl of sense robe and 10 μl of

antisense probe were added, and incubated for overnight at 4 °C). Then cells were collected for the biotin-based pull-down assay. YTHDF1 expression levels were analyzed by real-time PCR analysis and western blotting. **, *p* value < 0.01; ***, *p* value < 0.001.

D.YTHDF1 was up-regulated in Esophageal cancer cells compared with normal tissues (GEPIA data, Red box for tumor tissue, n = 182; gray box for normal tissue, n = 286).

E.There was no significant expression change of YTHDC1 in Esophageal cancer cells compared with normal tissues (GEPIA data, Red box for tumor tissue, n =182; gray box for normal tissue, n =286).

F.The real-time PCR analyzed in the top showed that the expression of YTHDF1 and AKT3 with YTHDF1 overexpression (YTHDF1-OE) and the agarose electrophoresis of the PCR products also shown. The western analyzed in the bottom showed that the expression of YTHDF1 and AKT3 with YTHDF1 overexpression (YTHDF1-OE).

G.The real-time PCR analyzed in the top showed that the expression of YTHDF1 and AKT3 with YTHDF1 knockdown (sh-YTHDF1) and the agarose electrophoresis of the PCR products also shown. The western analyzed in the bottom showed that the expression of YTHDF1 and AKT3 with YTHDF1 knockdown (sh-YTHDF1).

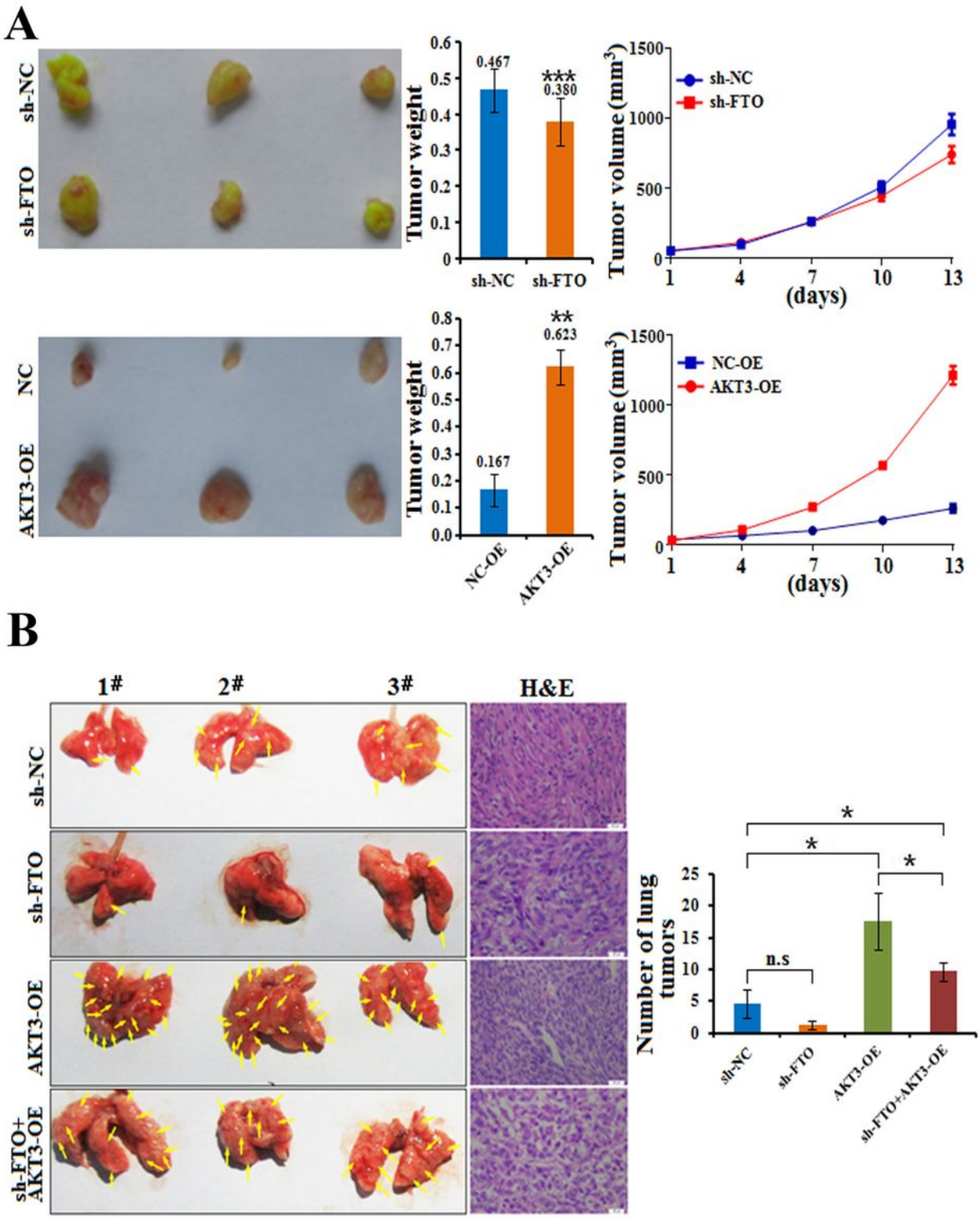

Figure 8

FTO and AKT3 promote esophageal cancer invasion *in vivo*.

A. FTO stable knock down or FTO stable expression cells were subcutaneously injected at two points at back of each nude mice, respectively. Representative images of the tumors on the 35th day of tumor formation, tumor weight and tumor growth curve of xenografts generated by FTO knockdown (sh-FTO)

and AKT3-expressing lentivirus (AKT3-OE) versus the negative control sh-NC and NC-OE, respectively (n = 3 for each group, **p< 0.01; ***p <0.001 by student t-test).

B. For the *in vivo* lung metastasis model, FTO stable knock down or FTO stable expression cells were subcutaneously injected into the nude mice by tail vein injection mice. WT (wild-type), sh-FTO, AKT3-OE and sh-FTO+AKT3-OE KYSE150 cells were injected (1×10^6 per mouse, n = 3 for each group). Six weeks after, mice were killed, and metastatic lung tumors were analyzed. Representative images of metastatic lung tumors and the H&E staining results were shown (left), and the number of lung tumors was quantitatively analyzed (right).

Supplementary Files

This is a list of supplementary files associated with this preprint. Click to download.

- Supplementarymaterials20220509.pdf